Study of the spatial correlation between neuronal activity and BOLD fMRI responses evoked by sensory and channelrhodopsin-2 stimulation in the rat somatosensory cortex

Nan Li[1,2], **Peter van Zijl**[1,2], **Nitish Thakor**[3], and **Galit Pelled**[1,2,*]

[1]F. M. Kirby Research Center for Functional Brain Imaging, Kennedy Krieger Institute, Baltimore, MD, United States

[2]The Russell H. Morgan Department of Radiology and Radiological Science, Johns Hopkins University School of Medicine, Baltimore, MD, United States

[3]The Department of Biomedical Engineering, Johns Hopkins University School of Medicine, Baltimore, MD, United States

Abstract

In this work we combined optogenetics tools with high-resolution blood oxygenation level dependent functional MRI (BOLD fMRI), electrophysiology, and optical imaging of cerebral blood flow (CBF), to study the spatial correlation between the hemodynamic responses and neuronal activity. We first investigated the spatial and temporal characteristics of BOLD fMRI and the underlying neuronal responses evoked by sensory stimulations at different frequencies. The results demonstrated that under dexmedetomidine anesthesia, BOLD fMRI and neuronal activity in the rat primary somatosensory cortex (S1) have different frequency - dependency and distinct laminar activation profiles. We the found that localized activation of channelrhodopsin-2 (ChR2) expressed in neurons throughout the cortex induced neuronal responses that were confined to the light stimulation S1 region (<500 μm) with distinct laminar activation profile. However, the spatial extent of the hemodynamic responses measured by CBF and BOLD fMRI induced by both ChR2 and sensory stimulation were greater than 3 mm. These results suggest that due to the complex neurovascular coupling it is challenging to determine specific characteristics of the underlying neuronal activity exclusively from the BOLD fMRI signals.

Introduction

Functional MRI (fMRI) techniques have rapidly grown in importance to enable characterization of the neuronal activity that occurs in the healthy brain and during pathology at the system level. Similar to other hemodynamics-based functional brain imaging techniques, the blood oxygenation level dependent (BOLD) fMRI signal is an indirect measurement of the neuronal activity. The exact relationship between the neuronal responses and hemodynamic responses remain unclear and under debates (Attwell et al.

*Corresponding author: Galit Pelled, Ph.D., Assistant Professor, F.M. Kirby Center for Functional Brain Imaging, Kennedy Krieger Institute, The Russell H. Morgan Department of Radiology and Radiological Science, Division of MR Research, Johns Hopkins University School of Medicine, 707 N Broadway, Baltimore, MD, 21205, Tel: 443-923-2751, Pelled@kennedykrieger.org.

2002; Logothetis 2008; Vanzetta et al. 2008; Enager et al. 2009; van Eijsden et al. 2009; Ekstrom 2010; Yen et al. 2011). Indeed, in recent years there have been great efforts to resolve this controversial topic. The vast majority of the microscopic research is focused on exploring the molecular factors implicated in the underlying neurovascular coupling, such as vasoactive ions, vasoactive factors related to energy metabolism, vasoactive factors/ neurotransmitters released by neuronal activation, and the role astrocytes play in neurovascular coupling (Lauritzen 2005; Iadecola et al. 2007; Devor et al. 2008; Koehler et al. 2009; Lecrux et al. 2011). The majority of the macroscopic research is focused on investigating the temporal correlation between the magnitude of the neuronal responses and the hemodynamic responses. Studies have demonstrated that the BOLD fMRI responses are tightly correlated to increases in local field potential (LFP) and spiking activity (Logothetis et al. 2001; Mukamel et al. 2005; Shmuel et al. 2006; Viswanathan et al. 2007; Kim et al. 2010); on the other hand, dissociation between LFP and spiking activity to hemodynamic responses has been reported (Caesar et al. 2003; Devor et al. 2007; Pelled et al. 2009; Lauritzen et al. 2012). In addition, the question of co-localization between BOLD responses and the corresponding neuronal activity remains difficult to address due to mechanism-based limitations in the MRI methodology.

The focus of this work was to investigate whether BOLD fMRI signal can be used to deduce about the underlying neuronal activity, and to what degree it co-localized with neuronal activity. Until recently, electrical stimulation via electrodes was used to map and modulate the stimulus response in the brain (Sultan et al. 2007). Optogenetics tools now enable neuronal manipulations that are precise, reversible and cell specific (Boyden et al. 2005; Zhang et al. 2010). These new tools provide the ability to elucidate detailed neuronal mechanisms associated with brain function. For example, optogenetics tools are being utilized to address questions regarding the basis of the neuronal activity that underlie the BOLD fMRI signals that were challenging to measure before (Lee et al. 2010; Desai et al. 2011; Kahn et al. 2011; Scott et al. 2012; Airan et al. 2013; Vazquez et al. 2013).

Conventional electrical forepaw stimulations were conducted to evoke neuronal firing rate in response to sensory afferent inputs through the thalamo-cortical circuits. We used optogenetics as a mean to produce localized stimulation of cortical neurons via optic fibers that have been demonstrated to not cause significant susceptibility effect that can interfere with MRI acquisition (Lee et al. 2010; Desai et al. 2011; Kahn et al. 2011; Li et al. 2011; Airan et al. 2013). A combination of multi-channel and micro-electrodes for electrophysiology recordings, optical imaging of cerebral blood flow (CBF) and BOLD fMRI were used to assess temporal and spatial characteristics of neuronal and hemodynamic responses. The results demonstrate that the BOLD fMRI, CBF, and neuronal responses in S1 evoked by sensory stimulation are frequency-dependent, have a distinct laminar profile and extend 3 mm along S1. The BOLD fMRI and CBF responses in S1 evoked by activation of channelrhodopsin-2 (ChR2) resulted in responses that were similar in their spatial extent to the one induced by conventional limb stimulation. However, the neuronal responses evoked by ChR2 stimulation were confined to the light stimulation region which was below 0.5 mm. Thus, it is manifested that it is plausible that under certain conditions the BOLD fMRI responses is only partially co-localized with the neuronal responses.

Materials and Methods

All animal procedures were conducted in accordance with the NIH *Guide for the Care and Use of Laboratory Animals* and approved by the Johns Hopkins University Animal Care and Use Committee.

Animal preparation

Lentivirus production and transduction were performed according to Gradinaru et al. (Gradinaru et al. 2009). The lentivirus (5 μl) containing Lenti-CaMKIIα-ChR2-EYFP-WPRE was delivered into the lateral ventricle to P3 rat pups as described previously (Li et al. 2011). Twenty-two rats expressing ChR2 were studied. Electrophysiology, optical imaging and fMRI measurements were performed on 10–11 weeks old rats expressing ChR2 (220 ± 50 g). For electrophysiology and fMRI measurement, a craniotomy (~1-mm square) was performed above the right S1 (centered at AP = −0.5 mm, ML = 3.7 mm, relative to Bregma). For optical imaging, the skull above right S1 (4 mm × 5 mm) was thinned to ~ 100 μm until the underlying cerebral vessels were visualized. After surgery, isoflurane was discontinued and a bolus of dexmedetomidine (0.05 mg/kg, S.C.) was given. The anesthesia was then maintained by a continuous infusion (0.1 mg/kg/hr) of dexmedetomidine (Zhao et al. 2008; Pawela et al. 2010). Respiration rate, oxygen saturation and heart rate were continuously monitored throughout all measurements by an oximeter (MouseOx, STARR Life Sciences Corp, PA, USA).

Forepaw stimulation

Electrical stimulation (World Precision Instruments, Sarasota, FL, USA) of the left forepaw was induced by two short electrodes that were inserted between the digits. The stimulation current was consisted of 3 mA, 300 μs pulses. Six different frequencies (1 Hz, 3 Hz, 6 Hz, 9 Hz, 20 Hz) were applied for 20 s respectively. After the frequency-dependency study, the maximum BOLD response frequency 9 Hz, as in agreement with previous studies (Zhao et al. 2008), was selected for the forepaw stimulation in the rest of experiments of this work.

ChR2 stimulation

A 3-foot long, 400-μm diameter optic fiber (0.39NA, FT400EMT, Thorlabs, Newton, NJ USA) was coupled to a 473 nm laser source (AL-473-60TA, Aixiz, Huston, TX USA) through a customized collimation setup. The other end of the optic fiber was mounted on top of the center of the right S1 craniotomy (AP = −0.5 mm, ML = 3.7 mm) without touching the brain tissue. The power of the light at the end of the optical fiber was measured with a digital optical power meter (PM100, Thorlabs, Newton, NJ USA). Various light intensities at the fiber output were tested in control rats not expressing ChR2, and 63.66 mW mm^{-2} was selected under which no significant cerebral blood flow and BOLD fMRI changes were observed in response to the light illumination. Light stimulation consisted of 20 ms of light pulses repeated at 20 Hz controlled by a shutter controller (SC10, Thorlabs, Newton, NJ USA) triggered via TTL signals which was generated and programmed using Spike 2 software (Cambridge Electronic Design. Cambridge, UK).

Electrophysiology recording

Extracellular neuronal activity recording was performed to determine the laminar S1 responses. A 12 channel axial array microelectrode with contacts spaced 150 μm apart (200 μm in diameter, 1 MΩ, FHC, Bowdoin, ME, USA) was used. The axial electrode was placed in the center of S1 (AP = −0.5 mm, ML = 3.7 mm), proximate to the optic fiber (<100 μm), and slowly lowered to the target depth using a micromanipulator (FHC).

In order to determine the spatial S1 responses, a customized grid of nine tungsten electrodes (125 μm in diameter with a tip size of a few micrometers, 350 KΩ, FHC, Bowdoin, ME, USA) was used. The tungsten electrodes were placed in a cross pattern and were spaced 500 μm apart. The whole grid covered a 2 mm × 2 mm area. The electrodes grid was lowered to the target depth (lamia IV; 700–800 μm below the pial surface) using a micromanipulator (FHC). The optic fiber was positioned proximate (<100 μm) to the center electrode in the grid (AP = −0.5 mm, ML = 3.7 mm).

Local field potential (LFP) and multi-unit activity (MUA) were sampled at 1k Hz and 11k Hz, and band-pass filtered between 0.1–500 Hz and 500 – 5k Hz, respectively. Discriminated signals were collected from a CED interface and Spike2 software (Cambridge Electronic Design, Cambridge UK). Three sets of data of 20 s forepaw or ChR2 stimulation were collected. To identify spiking events, the standard deviation (SD) of the MUA signals without stimulations was calculated for 5 s. MUA signals with amplitude greater than 4 times of the SD were defined as spiking activity. Post-stimulus time histogram (PSTH) analysis was performed to define stimulus evoked spiking activity. MUA that showed increased activity in one 5 ms bin during the first 40 ms following the onset of the stimulation were considered to show stimulus-evoked response. The number of stimulus-evoked spiking activity within the first 40 ms was calculated. LFP waveforms were averaged with respect to the stimulation triggers after removing the DC offset. The mean amplitude of the negative deflection was calculated for each train of stimuli. For LFP maps, data from the 12 contacts was resampled to 120 rows by using cubic spline interpolation.

Functional MRI

MRI Images were acquired on a 9.4 T horizontal MRI scanner (Bruker, Ettlingen, Germany). Rats were placed in a custom-built MRI rat cradle equipped with a dedicated holder for positioning the light source coupled MRI compatible optic fiber. A custom-built 1.1 cm diameter surface coil was used to transmit and receive MR signals (Airan et al. 2013). A gradient-echo, echo-planar imaging (GE EPI) sequence was used: echo time (TE) = 21 ms, repetition time (TR) = 1000 ms, bandwidth = 250 kHz, field of view (FOV) = 1.92 × 1.92 cm, matrix size= 128 × 128, resulting in an in plane resolution of 150 × 150 × 1000 μm. T2 weighted RARE sequence was used to acquire high resolution anatomical images with the following parameters: TE = 11 ms, TR = 2000 ms, number of averages = 2, band width =250 KHz, FOV = 1.92 × 1.92 cm, and matrix size = 256 × 256. Three coronal slices of images centered at Bregma 0 were acquired. Two epochs of 20 baseline and 20 scans during forepaw or ChR2 stimulation were collected. The FMRIB Software Library (FSL 4.1.9) software was used for analysis (Smith et al. 2004). Activation maps were obtained using the general linear model (GLM). The following pre-statistics processing was applied:

motion correction using FMRIB's Linear Image Registration Tool (MCFLIRT), grand-mean intensity normalization of the entire 4D dataset by a single multiplicative factor, and highpass temporal filtering (Gaussian-weighted least-squares straight line fitting, with sigma=30 s). The GLM method used in FMRI Expert Analysis Tool (FEAT) with local autocorrelation correction was used. Double-gamma hemodynamic response function (HRF) convolution kernel was applied to the basic event block to generate the design matrix. Z-score statistics were cluster-size thresholded for effective significance of $p<0.05$. The activation threshold was set at 2.3. Group and laminar analysis were performed by custom-written software running in MATLAB R2011b (MathWorks Inc., Natick, MA). In order to characterize the laminar BOLD fMRI signals, the surface of S1 forepaw representation (defined by a brain atlas) was defined by the user based on high resolution ($75 \times 75 \times 1000$ μm) RARE images. Three regions of interest (ROI) were defined: laminae II+III (150 μm– 600 μm), lamina IV (600 μm– 900 μm), and laminae V+VI (900 μm– 1800 μm). The number of activated voxels was calculated for each ROI. For each animal, laminar-specific BOLD fMRI response time courses were obtained by averaging all the active pixels from each ROI. We determined the spatial extent of the BOLD fMRI responses (within the medial-lateral axis) by calculating the number of active pixels along the ROI that represents lamia IV.

Optical imaging

Laser speckle contrast imaging (LSCI), a minimally invasive imaging modality, was used to collect CBF images with high spatiotemporal resolution (Dunn et al. 2001; Li et al. 2009). All raw laser speckle images were acquired using Basler piA640-210gm GigEvision camera (Basler Vision Technologies, Germany). A 60mm, f/2.8 macro-lens with a maximum reproduction ratio of 1:1 (Nikon Inc., Melville, NY) was mounted on the camera using a C mount to a Nikon F mount adapter. A 632 nm laser (0.5 mW, JDSU, Milpitas, CA) provided coherent illumination. A red light filter D620/30m (Chroma, Rokingham, Vermont, USA) was inserted between the camera and the lens to prevent 475nm light from entering the CCD sensor. A thinned-skull cranial window of 4 mm × 5 mm area centered at the right S1 was made for imaging. Before LSCI imaging, white light reflectance images were obtained to adjust the camera to focus on the cranial window area of interest under the illumination of a cold light source with fiber optics Luminator HGY3. Once the magnification of the camera was set, the aperture was set to the optimal condition for photographing speckles (Boas et al. 2010). The shutter speed was set to get an optimal exposure as 5 ms. Images were taken continuously at a rate of 25 frames per second. Software was written to control the image acquisition in LabView 2009 (National Instruments, Austin, TX, USA). Five sets of data from 20 s of baseline activity followed by 20 s of forepaw or ChR2 stimulation were collected. Raw speckle images were co-registered and the contrast was calculated according to Li et al. (Li et al. 2009). The intensity of LSCI contrast image is inversely proportional to the blood flow. Activation maps were obtained using two-tailed Z-test ($p<0.05$) with an activation threshold set to 3.5 and a cluster size of >10 pixels.

Immunohistochemistry

All rats were sacrificed and perfused at the end of the experiments to confirm ChR2 expression in pyramidal excitatory neurons. Free floating 50 μm thick coronal brain sections were immunostained with nuclear staining 4′,6-diamidino-2-phenylindole (DAPI, a nuclear

marker), anti- Enhanced Yellow Fluorescent Protein (EYFP, indicative of ChR2 expression) and anti-calcium/calmodulin-dependent protein kinase IIα (CaMKIIα, marker of excitatory pyramidal neurons) antibodies as described previously (Gradinaru et al. 2009). Images were acquired using a Zeiss microscope (Axio Imager M1 Stand Mot, Carl Zeiss Microscopy, LLC, Thornwood, NY, USA). In order to assess the number of neurons expressing ChR2, across 3 brain sections positioned at Bregma 0, 1, and 2, we counted the total number of DAPI stained cells (N_c) in S1. Since neurons consist of 63% of cortical cells (Miller et al. 1990) we calculated the total number of neurons (N_n). From the GFP staining results in these brain sections we counted the number of neurons that expressed ChR2 (N_ChR2). The percentage of neurons in S1 expressing ChR2 was calculated by 100* N_ChR2 /N_n.

Statistics

Two-tailed Student's *t* test was performed between the different stimulation conditions using Matlab (Mathworks). Results and figures show the average ± standard error of mean (SEM).

Results

Frequency-dependency of forepaw stimulus-evoked BOLD fMRI and neuronal responses

Electrical stimulation of the forepaw was applied to 11 rats. Six of them were tested in 9.4T MRI scanner to evaluate the forepaw stimulus-evoked BOLD fMRI responses. The activation Z-map of the BOLD fMRI responses was calculated by Z-test analysis with the effective significance of $p<0.05$. Electrophysiological recordings to measure the forepaw stimulus-evoked neuronal responses were tested on the other five rats. LFP and MUA were obtained throughout the depth of S1 by using the 12-channel axial array microelectrode positioned at the center of S1 forepaw representation (Bregma 0, ML 3.7 mm). Figure 1a shows activation Z-maps of the BOLD responses evoked by contralateral forepaw stimulations at 1 Hz, 3 Hz, 6 Hz, 9 Hz and 20 Hz. The highest amplitude of the BOLD fMRI percentage change averaged across S1 was observed at 9 Hz (6.45 ± 0.66 %, n=6), while the lowest value at 1 Hz (4.29 ± 0.59 %, n=6). The highest spatial extent of BOLD fMRI response, calculated by the number of the activated pixels in the functional Z-maps of BOLD signal, was observed at 6 Hz (327.17 ± 37.23, n=6). On the other hand, the highest amplitude of the stimulus - evoked LFP and MUA were observed at 3 Hz (1.87 ± 0.28 μV and 421.07 ± 58.13, respectively; n=5). These results demonstrate the different frequency - dependency of BOLD fMRI and neuronal responses of rats under dexmedetomidine anesthesia.

Laminar characteristics of forepaw stimulus-evoked BOLD fMRI and neuronal responses

Based on the above frequency-dependency results, the spatial comparison of signals were performed at 9 Hz, which was the frequency of where the greatest BOLD fMRI response was observed. The activated pixels, calculated by Z-test analysis of BOLD fMRI signals with effective significance of $p<0.05$, were found across the cortical depth in S1 contralateral to the forepaw stimulation. Three regions of interest (ROI) were defined: laminae II+III (150 – 600 μm), lamina IV (600 – 900 μm), and laminae V+IV (900 - 1800 μm). The time course and the amplitude of BOLD fMRI responses were calculated for each ROI. The increases of the BOLD fMRI signal occurred immediately following the

stimulation onset and persisted throughout the duration of the stimulation (Figure 2a). The highest amplitude of the BOLD fMRI percentage change was observed in laminae II+III (7.72 ± 0.48 %), followed by lamina IV (7.66 ± 0.44 %) and laminae V+VI (4.31 ± 0.14 %; n=6). The highest amplitude of the stimulus-evoked LFP and MUA were found in laminar IV (LFP: laminae II+III 0.26 ± 0.04 μV, lamina IV 1.49 ± 0.13 μV, laminae V+VI 1.04 ± 0.11 μV; MUA: laminae II+III 230.22 ± 28.53; lamina IV 454.68 ± 26.91; laminae V+VI 287.01 ± 30.69; n=5). Figure 2b and 2c show a representative example and the group averages of the laminar spatial distribution of the electrophysiology responses, respectively. In agreement with previous reports (Silva et al. 2002), we also observed differences in the spatial distribution of the responses between imaging and electrophysiology.

Lateral spatial profiles of forepaw stimulus-evoked BOLD fMRI and neuronal responses

After comparing the laminar characteristics of forepaw stimulus - evoked BOLD fMRI and neuronal responses, we then investigated how these neuronal responses are co-localized with the accompanying hemodynamic responses in the lateral spatial extent. Both BOLD fMRI and cerebral blood flow (CBF) responses were measured to evaluate the hemodynamic changes in S1 evoked by forepaw stimulation. Laser speckle contrast imaging (LSCI), a minimally invasive optical imaging method (Dunn et al. 2001; Li et al. 2009), was performed to detect CBF responses in S1 representation (FOV = 3.75 × 5.1 mm). This technique is sensitive to CBF changes of the upstream pial arterioles and draining venules within a cortical depth of approximately 0.6–0.8 mm (Dunn et al. 2005). The lateral spatial extent of the CBF Z-maps responses revealed by LSCI (Z-test analysis with effective significance of p<0.05) to forepaw stimulation were observed across FOV that covered the right S1 forepaw representation (n=5) (Figure 3a). The percent change of the BOLD fMRI responses across the activated pixels within lamina IV was calculated for each individual animal for each condition, and averaged across subjects (n=6). Consistent with the direct optical CBF measurements, the spatial extents of the BOLD fMRI Z-maps responses to forepaw covered a region in medial-lateral distance of 3,600 ± 198 μm (Figure 3b).

The lateral spatial characteristics of neuronal responses evoked by forepaw stimulation were tested by a grid of nine tungsten electrodes. This grid covered a 2 × 2 mm area within the S1 forepaw representation (Figure 3c). LFP and MUA responses were recorded simultaneously from all nine electrodes that were lowered into lamina IV Forepaw stimulation resulted in LFP and MUA responses that were detected in all the electrodes positioned across the right S1 representation (Figure 3d and 3e).

Spatial activation profiles of optogenetics-induced BOLD fMRI and neuronal responses

To further investigate the co-localization between the BOLD fMRI and neuronal responses, we induced localized neuronal activation by optogenetics approaches. Fifteen animals were genetically engineered to express ChR2 in excitatory cortical neurons. Immunohistochemistry was performed on brain slices obtained from all the rats that participated in this study (Figure 4a). Cells that were positively stained for DAPI (nuclear staining), EYFP (indicative of ChR2 expression) and CaMKIIα (marker for excitatory neurons) were found across the cortical depth at laminae II to VI in S1 granular zone and consisted about 35% of all neurons in that area. An optical fiber was used for light delivery

and laser pulses of 20 Hz for 20 ms were applied to produce reproducible neuronal responses (Gradinaru et al. 2009; Lee et al. 2010).

Figure 4b shows the laminar activation profiles of the LFP responses in S1 that were evoked by the ChR2 stimulation. The neuronal responses were confined to lamina IV (with the peak LFP amplitude of 0.12 ± 0.02 μV) and the supragranular laminae with response amplitudes 10 times smaller compared to forepaw stimulation (Student t-test, p<0.005, n=5). Figure 4c and 4d demonstrate the lateral spatial profiles of the LFP and MUA responses across lamina IV of S1 that were measured by 9-channel electrodes grid. Both evoked LFP and MUA responses by ChR2 stimulation were detected only in the electrode proximate (<100 μm) to the optic fiber that delivered the light stimulation, with minimal evoked responses in the other eight electrodes (Figure 4c and 4d). Thus, the ChR2 stimulation resulted in neuronal responses that were limited to laminar IV and II+III with a spatial extent of less than 500 μm.

We then characterized the spatial characteristics of the hemodynamic responses evoked by ChR2 stimulations across the forepaw representation in S1. Although the changes in neuronal firing rate induced by ChR2 stimulation, as demonstrated above, were localized to the stimulated cortical area, the hemodynamic responses were found to cover a much broader area and were only partially co-localized with the underlying neuronal responses (Figure 4e and 4f). The extents of the CBF Z-maps responses to ChR2 stimulations in S1 were observed across the FOV that covered the S1 forepaw representation ($3,700 \pm 233$ μm vs. $3,750 \pm 180$ μm, n=5; Figure 4g). The average amplitude of the CBF responses across S1 was about two times less in response to ChR2 stimulation compared to forepaw stimulation (15.07 ± 2.12 % vs. 28.40 ± 1.75 %; Student t-test, p<0.005, n=5). Consistent with the direct optical CBF measurements, the spatial extents of the BOLD fMRI Z-maps responses to ChR2 stimulation were similar to the activation maps obtained following forepaw stimulation ($3,450 \pm 244$ μm vs. $3,600 \pm 198$ μm, n=5; Figure 4h). The average amplitude of the BOLD responses across the activated pixels within S1 was two times less in response to ChR2 compared to forepaw stimulation (2.49 ± 0.54 % vs. 5.51 ± 0.26 %; Student t-test, p<0.05, n=5). We also characterized the laminar profiles of BOLD fMRI responses to the ChR2 stimulation (Figure 4i). The highest BOLD fMRI increases were detected in laminae II+III, followed by lamina IV and lamina V+VI, which were similar to the laminar activation profiles observed as a response to forepaw stimulation.

Discussion

We studied the relationship between the neuronal and BOLD fMRI responses in the somatosensory cortex by comparing neuronal and hemodynamic responses evoked by sensory and localized ChR2 stimulations. Multi-model measurements including multi-channel electrophysiology recordings, optical imaging of CBF and BOLD fMRI were applied. In agreement with previous studies (Sanganahalli et al. 2008; Kim et al. 2010), the evoked neuronal and its accompanying BOLD fMRI responses to tactile stimulation demonstrated differences in their stimulus frequency-dependency and laminar characteristics. We than sought to further investigate the spatial co-localization of the neuronal and hemodynamic responses by using optogenetics as a mean to activate a

localized subset of S1 neurons. The results demonstrated that stimulation of ChR2-expressing excitatory neurons in S1 induced neuronal activity that was mainly confined to lamina IV. However, the extent of the CBF and BOLD fMRI hemodynamic responses due to ChR2 stimulation were greater than the neuronal activity measured by electrophysiology and similar to the hemodynamic responses evoked by tactile stimulation.

The neuronal pathway by which peripheral tactile stimulation activates cortical neuronal assemblies and its activation patterns across the cortical laminae and the somatosensory representation is well described. Recently several studies using transgenic mice expressing ChR2 in excitatory neurons in lamina V of sensory and motor cortices focused on the correlation between the neuronal and the hemodynamic responses (Lee et al. 2010; Desai et al. 2011; Kahn et al. 2011; Scott et al. 2012; Kahn et al. 2013; Vazquez et al. 2013). These studies have demonstrated high temporal linearity and correlation between the BOLD fMRI responses due to the optogenetics stimulation and the neurophysiological measured responses. However, unlike neuronal responses evoked by tactile sensory stimulation that are known to initiate in lamina IV, Both Khan et al (Kahn et al. 2013) and Vazquez et al (Vazquez et al. 2013) reported that the maximal neuronal activity observed in the transgenic mice that express ChR2 specifically in lamina V, was detected in lamina V.

The principal difference between our animal model to the above studies is that in our study, the ChR2 was expressed throughout the cortical depth of the rat's brain, and was not confined to deep cortical laminae. Consequently, we could induce ChR2 activity in supragranular laminae and elicit localized neuronal activity in lamina IV, which is also the primary lamina receiving thalamo-cortical projections and responding to thalamo-cortical input. This has led to cortical responses that exhibited different neuronal characteristics compared to conventional tactile stimulation in terms of the neuronal activity distribution across the cortical depth and the somatosensory representation. Nevertheless, it produced hemodynamic responses that had similar characteristics to the ones detected following tactile stimulation. Interestingly, a recent study demonstrated that administration of glutamate receptor antagonists significantly decreased sensory evoked hemodynamic responses, but had little effect on ChR2 evoked hemodynamic responses in transgenic mice expressing ChR2 in lamina V (Scott et al. 2012). These findings further support that hemodynamic responses may be independent of local excitatory synaptic transmission. Together, these findings suggest a fundamental difference in the spatial extent between the neuronal and the hemodynamic responses, and that under certain conditions the BOLD fMRI responses may only partially co-localized with the neuronal responses.

Simultaneous electrophysiology recordings and fMRI measurements in the cat's visual cortex (Kim et al. 2004) demonstrated that the BOLD fMRI signals that were averaged across millimeters scale were tightly correlated to the electrophysiological responses. However, BOLD fMRI signals that were averaged for voxel sizes smaller than 2.6×2.6 mm^2 showed high variance and correlation of less than 50% with the electrophysiological responses. It emerges that the spatial correspondence between BOLD fMRI, optical imaging and neuronal activity is determined by intrinsic properties of both the neurovascular coupling mechanism and the imaging technologies. BOLD fMRI signals originate from partially deoxygenated blood vessels, such as capillaries, venules and downstream veins

(Davis et al. 1998; van Zijl et al. 1998), while optical CBF imaging generally detects blood flow in arterioles and upstream pia arteries (Li et al. 2009; Boas et al. 2010). Gradient echo (GE) pulse sequence, as was used in this study, is the common BOLD fMRI method. However, the GE-BOLD fMRI signals are highly sensitive for large draining veins which reduce the capability of the technology to detect neuronal responses in submillimeter resolution (Zhao et al. 2006). Other methods such as spin echo BOLD fMRI, cerebral blood volume and cerebral blood flow MRI measurements may provide superior spatial localization of neuronal activities (Ugurbil et al. 2003; Zhao et al. 2004; Moon et al. 2007). However, they offer lower temporal resolution and signal-to-noise ratios compare to the GE-BOLD fMRI method and are therefore less applied in functional brain studies (Kim et al. 2012).

In our study, even though the neuronal responses as a result of ChR2 stimulation were found to be localized in electrodes adjacent to the light stimulation area, the accompanying hemodynamic changes were detected more than 3 mm further in S1. Capitalizing on previous studies, the results suggest that due to the complex hemodynamic mechanism that is the basis of the BOLD fMRI contrast there may be differences in the spatial extent between the neuronal and the hemodynamic responses.

Acknowledgments

References

Airan RD, Li N, Gilad AA, Pelled G. Genetic tools to manipulate MRI contrast. NMR Biomed. 2013; 26:803–809. [PubMed: 23355411]

Attwell D, Iadecola C. The neural basis of functional brain imaging signals. Trends Neurosci. 2002; 25:621–625. [PubMed: 12446129]

Boas DA, Dunn AK. Laser speckle contrast imaging in biomedical optics. J Biomed Opt. 2010; 15:011109. [PubMed: 20210435]

Boyden ES, Zhang F, Bamberg E, Nagel G, Deisseroth K. Millisecond-timescale, genetically targeted optical control of neural activity. Nat Neurosci. 2005; 8:1263–1268. [PubMed: 16116447]

Caesar K, Thomsen K, Lauritzen M. Dissociation of spikes, synaptic activity, and activity-dependent increments in rat cerebellar blood flow by tonic synaptic inhibition. Proc Natl Acad Sci U S A. 2003; 100:16000–16005. [PubMed: 14673091]

Davis TL, Kwong KK, Weisskoff RM, Rosen BR. Calibrated functional MRI: mapping the dynamics of oxidative metabolism. Proc Natl Acad Sci U S A. 1998; 95:1834–1839. [PubMed: 9465103]

Desai M, Kahn I, Knoblich U, Bernstein J, Atallah H, Yang A, et al. Mapping brain networks in awake mice using combined optical neural control and fMRI. J Neurophysiol. 2011; 105:1393–1405. [PubMed: 21160013]

Desai M, Kahn I, Knoblich U, Bernstein J, Atallah H, Yang A, et al. Mapping brain networks in awake mice using combined optical neural control and fMRI. J Neurophysiol. 2011; 105:1393–1405. [PubMed: 21160013]

Devor A, Hillman EM, Tian P, Waeber C, Teng IC, Ruvinskaya L, et al. Stimulus-induced changes in blood flow and 2-deoxyglucose uptake dissociate in ipsilateral somatosensory cortex. J Neurosci. 2008; 28:14347–14357. [PubMed: 19118167]

Devor A, Tian P, Nishimura N, Teng IC, Hillman EM, Narayanan SN, et al. Suppressed neuronal activity and concurrent arteriolar vasoconstriction may explain negative blood oxygenation level-dependent signal. J Neurosci. 2007; 27:4452–4459. [PubMed: 17442830]

Dunn AK, Bolay H, Moskowitz MA, Boas DA. Dynamic imaging of cerebral blood flow using laser speckle. J Cereb Blood Flow Metab. 2001; 21:195–201. [PubMed: 11295873]

Dunn AK, Devor A, Dale AM, Boas DA. Spatial extent of oxygen metabolism and hemodynamic changes during functional activation of the rat somatosensory cortex. Neuroimage. 2005; 27:279–290. [PubMed: 15925522]

Ekstrom A. How and when the fMRI BOLD signal relates to underlying neural activity: the danger in dissociation. Brain Res Rev. 2010; 62:233–244. [PubMed: 20026191]

Enager P, Piilgaard H, Offenhauser N, Kocharyan A, Fernandes P, Hamel E, et al. Pathway-specific variations in neurovascular and neurometabolic coupling in rat primary somatosensory cortex. J Cereb Blood Flow Metab. 2009; 29:976–986. [PubMed: 19337274]

Gradinaru V, Mogri M, Thompson KR, Henderson JM, Deisseroth K. Optical deconstruction of parkinsonian neural circuitry. Science. 2009; 324:354–359. [PubMed: 19299587]

Iadecola C, Nedergaard M. Glial regulation of the cerebral microvasculature. Nat Neurosci. 2007; 10:1369–1376. [PubMed: 17965657]

Kahn I, Desai M, Knoblich U, Bernstein J, Henninger M, Graybiel AM, et al. Characterization of the functional MRI response temporal linearity via optical control of neocortical pyramidal neurons. J Neurosci. 2011; 31:15086–15091. [PubMed: 22016542]

Kahn I, Knoblich U, Desai M, Bernstein J, Graybiel AM, Boyden ES, et al. Optogenetic drive of neocortical pyramidal neurons generates fMRI signals that are correlated with spiking activity. Brain Res. 2013; 1511:33–45. [PubMed: 23523914]

Kim DS, Ronen I, Olman C, Kim SG, Ugurbil K, Toth LJ. Spatial relationship between neuronal activity and BOLD functional MRI. Neuroimage. 2004; 21:876–885. [PubMed: 15006654]

Kim SG, Ogawa S. Biophysical and physiological origins of blood oxygenation level-dependent fMRI signals. J Cereb Blood Flow Metab. 2012; 32:1188–1206. [PubMed: 22395207]

Kim T, Masamoto K, Fukuda M, Vazquez A, Kim SG. Frequency-dependent neural activity, CBF, and BOLD fMRI to somatosensory stimuli in isoflurane-anesthetized rats. Neuroimage. 2010; 52:224–233. [PubMed: 20350603]

Koehler RC, Roman RJ, Harder DR. Astrocytes and the regulation of cerebral blood flow. Trends Neurosci. 2009; 32:160–169. [PubMed: 19162338]

Lauritzen M. Reading vascular changes in brain imaging: is dendritic calcium the key? Nat Rev Neurosci. 2005; 6:77–85. [PubMed: 15611729]

Lauritzen M, Mathiesen C, Schaefer K, Thomsen KJ. Neuronal inhibition and excitation, and the dichotomic control of brain hemodynamic and oxygen responses. Neuroimage. 2012; 62:1040–1050. [PubMed: 22261372]

Lecrux C, Hamel E. The neurovascular unit in brain function and disease. Acta Physiol (Oxf). 2011; 203:47–59. [PubMed: 21272266]

Lee JH, Durand R, Gradinaru V, Zhang F, Goshen I, Kim DS, et al. Global and local fMRI signals driven by neurons defined optogenetically by type and wiring. Nature. 2010; 465:788–792. [PubMed: 20473285]

Li N, Downey JE, Bar-Shir A, Gilad AA, Walczak P, Kim H, et al. Optogenetic-guided cortical plasticity after nerve injury. Proc Natl Acad Sci U S A. 2011; 108:8838–8843. [PubMed: 21555573]

Li N, Jia X, Murari K, Parlapalli R, Rege A, Thakor NV. High spatiotemporal resolution imaging of the neurovascular response to electrical stimulation of rat peripheral trigeminal nerve as revealed by in vivo temporal laser speckle contrast. J Neurosci Methods. 2009; 176:230–236. [PubMed: 18706442]

Logothetis NK. What we can do and what we cannot do with fMRI. Nature. 2008; 453:869–878. [PubMed: 18548064]

Logothetis NK, Pauls J, Augath M, Trinath T, Oeltermann A. Neurophysiological investigation of the basis of the fMRI signal. Nature. 2001; 412:150–157. [PubMed: 11449264]

Miller MW, Potempa G. Numbers of neurons and glia in mature rat somatosensory cortex: effects of prenatal exposure to ethanol. J Comp Neurol. 1990; 293:92–102. [PubMed: 2312794]

Moon CH, Fukuda M, Park SH, Kim SG. Neural interpretation of blood oxygenation level-dependent fMRI maps at submillimeter columnar resolution. J Neurosci. 2007; 27:6892–6902. [PubMed: 17596437]

Mukamel R, Gelbard H, Arieli A, Hasson U, Fried I, Malach R. Coupling between neuronal firing, field potentials, and FMRI in human auditory cortex. Science. 2005; 309:951–954. [PubMed: 16081741]

Pawela CP, Biswal BB, Hudetz AG, Li R, Jones SR, Cho YR, et al. Interhemispheric neuroplasticity following limb deafferentation detected by resting-state functional connectivity magnetic resonance imaging (fcMRI) and functional magnetic resonance imaging (fMRI). Neuroimage. 2010; 49:2467–2478. [PubMed: 19796693]

Pelled G, Bergstrom DA, Tierney PL, Conroy RS, Chuang KH, Yu D, et al. Ipsilateral cortical fMRI responses after peripheral nerve damage in rats reflect increased interneuron activity. Proc Natl Acad Sci U S A. 2009; 106:14114–14119. [PubMed: 19666522]

Sanganahalli BG, Herman P, Hyder F. Frequency-dependent tactile responses in rat brain measured by functional MRI. NMR Biomed. 2008; 21:410–416. [PubMed: 18435491]

Scott NA, Murphy TH. Hemodynamic responses evoked by neuronal stimulation via channelrhodopsin-2 can be independent of intracortical glutamatergic synaptic transmission. PLoS One. 2012; 7:e29859. [PubMed: 22253807]

Shmuel A, Augath M, Oeltermann A, Logothetis NK. Negative functional MRI response correlates with decreases in neuronal activity in monkey visual area V1. Nat Neurosci. 2006; 9:569–577. [PubMed: 16547508]

Silva AC, Koretsky AP. Laminar specificity of functional MRI onset times during somatosensory stimulation in rat. Proc Natl Acad Sci U S A. 2002; 99:15182–15187. [PubMed: 12407177]

Smith SM, Jenkinson M, Woolrich MW, Beckmann CF, Behrens TE, Johansen-Berg H, et al. Advances in functional and structural MR image analysis and implementation as FSL. Neuroimage. 2004; 23(Suppl 1):S208–219. [PubMed: 15501092]

Sultan F, Augath M, Logothetis N. BOLD sensitivity to cortical activation induced by microstimulation: comparison to visual stimulation. Magn Reson Imaging. 2007; 25:754–759. [PubMed: 17482409]

Ugurbil K, Toth L, Kim DS. How accurate is magnetic resonance imaging of brain function? Trends Neurosci. 2003; 26:108–114. [PubMed: 12536134]

van Eijsden P, Hyder F, Rothman DL, Shulman RG. Neurophysiology of functional imaging. Neuroimage. 2009; 45:1047–1054. [PubMed: 18801442]

van Zijl PC, Eleff SM, Ulatowski JA, Oja JM, Ulug AM, Traystman RJ, et al. Quantitative assessment of blood flow, blood volume and blood oxygenation effects in functional magnetic resonance imaging. Nat Med. 1998; 4:159–167. [PubMed: 9461188]

Vanzetta I, Grinvald A. Coupling between neuronal activity and microcirculation: implications for functional brain imaging. HFSP J. 2008; 2:79–98. [PubMed: 19404475]

Vazquez AL, Fukuda M, Crowley JC, Kim SG. Neural and Hemodynamic Responses Elicited by Forelimb- and Photo-stimulation in Channelrhodopsin-2 Mice: Insights into the Hemodynamic Point Spread Function. Cereb Cortex. 2013

Viswanathan A, Freeman RD. Neurometabolic coupling in cerebral cortex reflects synaptic more than spiking activity. Nat Neurosci. 2007; 10:1308–1312. [PubMed: 17828254]

Yen CC, Fukuda M, Kim SG. BOLD responses to different temporal frequency stimuli in the lateral geniculate nucleus and visual cortex: insights into the neural basis of fMRI. Neuroimage. 2011; 58:82–90. [PubMed: 21704712]

Zhang F, Gradinaru V, Adamantidis AR, Durand R, Airan RD, de Lecea L, et al. Optogenetic interrogation of neural circuits: technology for probing mammalian brain structures. Nat Protoc. 2010; 5:439–456. [PubMed: 20203662]

Zhao F, Wang P, Hendrich K, Ugurbil K, Kim SG. Cortical layer-dependent BOLD and CBV responses measured by spin-echo and gradient-echo fMRI: insights into hemodynamic regulation. Neuroimage. 2006; 30:1149–1160. [PubMed: 16414284]

Zhao F, Wang P, Kim SG. Cortical depth-dependent gradient-echo and spin-echo BOLD fMRI at 9.4T. Magn Reson Med. 2004; 51:518–524. [PubMed: 15004793]

Zhao F, Zhao T, Zhou L, Wu Q, Hu X. BOLD study of stimulation-induced neural activity and resting-state connectivity in medetomidine-sedated rat. Neuroimage. 2008; 39:248–260. [PubMed: 17904868]
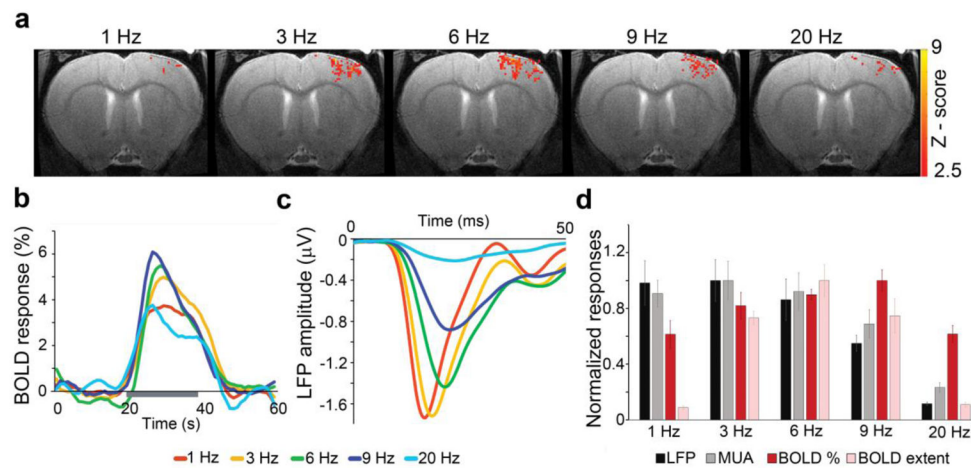
Figure 1. BOLD fMRI and neuronal activity evoked by sensory stimulation have different frequency-dependency in S1

a. Examples of BOLD fMRI activation maps in response to contralateral forepaw stimulation at 1 Hz, 3 Hz, 6 Hz, 9 Hz and 20 Hz. **b.** Averaged time courses of BOLD fMRI percentage changes in response to forepaw stimulation at different frequencies (mean, n=6). The gray color bar depicts the length of stimulation. **c.** Averaged time courses and amplitudes of LFP in response to forepaw stimulation at different frequencies (mean, n=5). **d.** Normalized group results (mean ± SEM) showed that the maximal magnitude of LFP and the spiking rate of MUA (n=5) was observed when the stimulus was presented at 3 Hz, while the peak of the BOLD fMRI percentage change and its extent was observed at 9 Hz and 6 Hz, respectively (n=6).
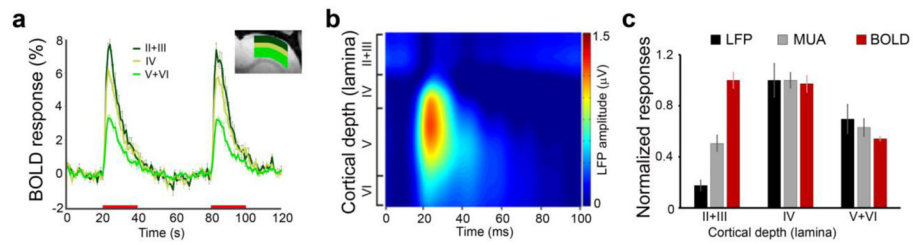
Figure 2. BOLD fMRI and neuronal activity evoked by sensory stimulation at 9 Hz have different laminar profile

a. Time courses and amplitudes of BOLD fMRI responses to forepaw stimulation across the cortical depth (mean ± SEM; n=6) demonstrate that hemodynamic responses initiated and had the highest amplitude in laminae II+III. **b.** Example of evoked LFP responses to forepaw stimulation demonstrates that neuronal responses initiated and had the highest amplitude in lamina IV, and then spread throughout the cortical depth. **c.** Normalized group results (mean ± SEM) of averaged LFP amplitude (n=5), spiking rates of MUA (n=5), and magnitude of BOLD fMRI (n=6) responses across the cortical depth.
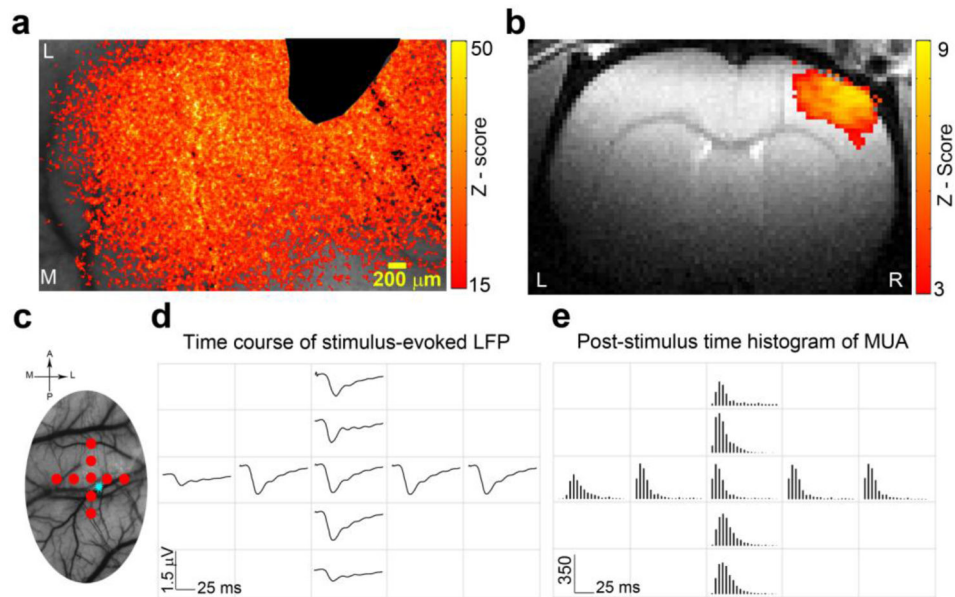
Figure 3. Hemodynamic responses and neuronal activity evoked by sensory stimulation have similar spatial extent across S1

a. Examples of CBF activation z-map overlaid on the original CBF contrast images show that both forepaw and ChR2 stimulations resulted in extensive hemodynamic responses in the right S1. The tip of the optic fiber used for ChR2 was masked off from the images. **b.** Examples of BOLD fMRI activation z-map overlaid on the anatomical images. **c.** An illustration of the position of the nine recording electrodes (red dots) and the optic fiber (blue star) overlaid on a LSCI image of the rat S1. **d.** Forepaw stimulation resulted in LFP responses that were observed in all nine electrodes that were positioned at lamia IV and covered 2 mm × 2 mm of S1. **e.** Forepaw stimulation resulted in MUA that were observed in all nine electrodes across S1.
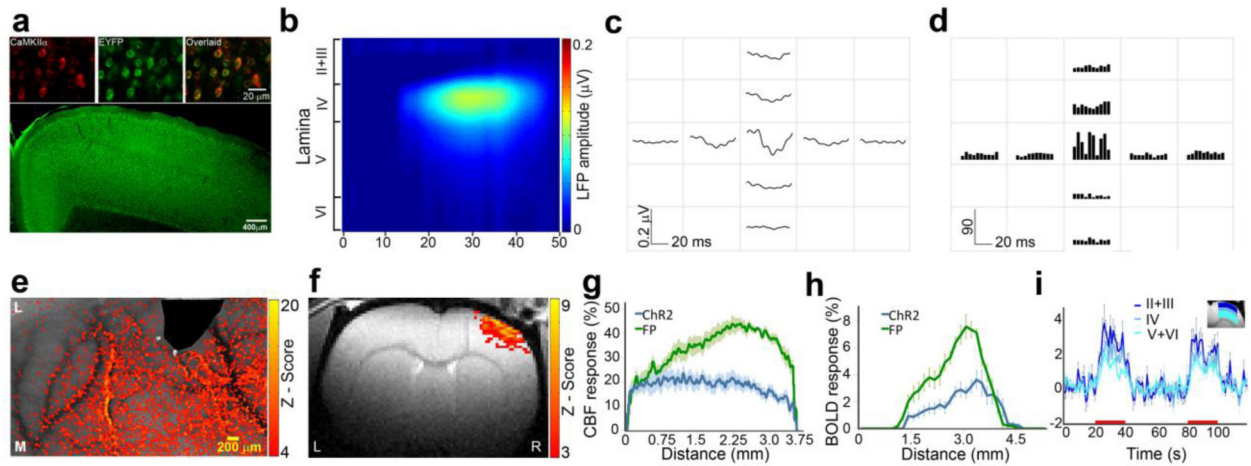
Figure 4. Hemodynamic responses and neuronal activity evoked by ChR2 stimulation are partially co-localized in S1

a. Examples of neurons within S1 immunostained with antibodies targeted towards EYFP (green, indicative of ChR2 expression) and CaMKIIα (red, marker of excitatory pyramidal neurons). A large field of view fluorescence image shows that ChR2 expressing neurons are located throughout the cortex. **b.** Example of evoked LFP responses to ChR2 stimulation shows that responses were confined to laminae II+III and IV. **c.** ChR2 stimulation resulted in evoked LFP responses that were observed only in electrodes proximate to the optic fiber with a distance less than 500 μm. **d.** ChR2 stimulation resulted in increased MUA spiking activities only in electrodes proximate to the optic fiber. **e.** Example of CBF activation z-map shows that ChR2 stimulations resulted in extensive CBF increases in S1. **f.** Example of BOLD fMRI activation z-map shows that ChR2 stimulations resulted in extensive BOLD fMRI responses in S1. **g.** Group average of the CBF responses across S1 representation (in the medial-lateral axis) demonstrates similar spatial extent of the hemodynamic responses induced by forepaw and ChR2 stimulations (mean ± SEM, n=5). **h.** Group average of the BOLD fMRI responses across lamina IV S1 representation (in the medial-lateral axis) demonstrates similar extent and localization of the hemodynamic responses induced by forepaw and ChR2 stimulations (mean ± SEM, n=5). **I.** Time courses of BOLD fMRI responses across the cortical laminae evoked by ChR2 (mean ± SEM, n=5).